Sensors and Actuators B 239 (2017) 397–404

Contents lists available at ScienceDirect

Sensors and Actuators B: Chemical

journal homepage: www.elsevier.com/locate/snb

Automatic generation of photochemically induced excitation-emission-kinetic four-way data for the highly selective determination of azinphos-methyl in fruit juices

Milagros Montemurro, Gabriel G. Siano, María J. Culzoni*, Héctor C. Goicoechea*

Universidad Nacional del Litoral-CONICET, Facultad de Bioquímica y Ciencias Biológicas, Laboratorio de Desarrollo Analítico y Quimiometría (LADAQ), Ciudad Universitaria, 3000, Santa Fe, Argentina

ARTICLE INFO

Article history:
Received 21 June 2016
Received in revised form 28 July 2016
Accepted 7 August 2016
Available online 8 August 2016

Keywords:
Azinphos-methyl
Photochemically induced degradation
Four-way data
Fruit juice

ABSTRACT

An application of four-way multivariate calibration for the quantitation of azinphos-methyl (AZM) in fruits is presented. The known photochemically induced degradation of AZM into a highly fluorescent product was exploited for the generation of third-order data with quantitative purpose. The data generation consisted in the measurement of excitation-emission fluorescence matrices at different times after UV-light irradiation. For this purpose, a reactor was built connecting an external UV-light source through an optical fiber to the sample holder. The data were modelled with two algorithms, PARAFAC and U-PLS/RTL. The second-order advantage was exploited in the analysis of samples containing un-modelled components and an improvement in the analytical figures of merit was observed as long as the data dimensions were increased. The method was successfully applied to the quantitation of AZM in apple, pear and peach juice samples with and without spiked analyte. The limits of detection were of 3.6 $\mu g\,L^{-1}$ in aqueous solution and 21–66 $\mu g\,L^{-1}$ in fruit juice samples.

1. Introduction

Although the use of pesticides provides benefits to the agriculture industry, their incorrect application may leave harmful residues, which involves possible health risks. The concentration of pesticides is regulated in many samples such as drinking waters, vegetables, juices, etc., by the European Commission [1] and the Food and Drug Administration [2], among other agencies. In Argentina, the National Service of Health and Agrifood Quality (SENASA), which is responsible for the registration, use and regulation of pesticides, sets the maximum residue levels (MRLs), i.e. the highest level of a pesticide residue that is legally tolerated in or on food or feed when pesticides are applied correctly [1,3].

Azinphos-methyl (AZM) is an organophosphate insecticide and acaricide, widely and efficiently used to protect pomes (apple and pear), drupe (peach, plum and cherry) and nut trees from a variety of insects. AZM presents a weak natural fluorescence in aqueous solution, which can be enhanced in a variety of ways, including UV photolysis, inclusion into cyclodextrins, and base hydrolysis [4]. There are previous studies related to the photochemistry of this important pesticide, in which different mechanisms have been proposed [4–6]. L. Yeasmin et al. have described a detailed UV-A photolysis mechanism involving two pathways, the major one leading to benzazimide as the stable photoproduct, and the other to N-methylanthranilic acid as an intermediate and aniline as a final stable photoproduct [7]. On the other hand, a base-catalysed conversion of AZM to anthranilic acid has been used to its detection in a fluorescence-based trace analysis [8].

A comprehensive search and the analysis of the reported methods for the determination of AZM evidenced a variety of techniques requiring, in their majority, highly sophisticated equipment. Among them, high performance liquid chromatography-diode array detector (HPLC-DAD) [9], liquid chromatography triple quadrupole tandem mass spectrometry (LC-QqQ-MS/MS) [10], gas chromatography-tandem mass spectrometry (GC–MS/MS) [11,12], gas chromatography-nitrogen phosphorous detection (GC-NPD) [13,14] and micellar electrokinetic chromatography (MEKC) [15] can be mentioned. Considering these techniques provide good and reliable results, the aim was to achieve such satisfactory performance but using a simpler and more accessible technique, as it is fluorescence spectroscopy, and to make an extra contribution to the method outcome by using higher dimension data and multiway calibration.

* Corresponding authors.
E-mail addresses: mculzoni@fbcb.unl.edu.ar (M.J. Culzoni), hgoico@fbcb.unl.edu.ar (H.C. Goicoechea).

http://dx.doi.org/10.1016/j.snb.2016.08.033
0925-4005/

In analytical chemistry, the use of higher order data has been increased due to the current technological development. There is an improvement in the selectivity and sensitivity of the analysis when the data dimension is augmented, which provides additional sample information. Furthermore, the second-order advantage is achieved with second- and higher-order data and enables the accurate quantitation of the calibrated analytes in the presence of non-modelled substances [16].

Introducing an extra data dimension to a second-order data leads to third-order data, and the mathematical object obtained by grouping third-order data for several samples into the fourth dimension is known as a four-way array [17]. Fluorescence spectroscopy, a technique widely applied in chemical and biological sciences, is highly sensitive and allows obtaining four-way data by introducing additional dimensions [18]. Different strategies, such as recording the excitation–emission fluorescence matrix (EEFM) as a function of pH [18,19] or volume of quencher [20], and time evolution of EEFM data while following the kinetics of a reaction [21–27], have been reported.

Several algorithms, such as parallel factor analysis (PARAFAC) [28,29], multivariate curve resolution alternating least squares (MCR-ALS) [29], unfolded partial least squares and multi-way partial least squares combined with residual trilinearization (U-PLS/RTL, N-PLS/RTL) [24,28–30], alternating quadrilinear decomposition (AQLD) and alternating weighted residue constraint quadrilinear decomposition (AWRCQLD) [31], among others, are available for the analysis of four-way data tensors.

In the present work, we report a fluorescent kinetic method for the determination of AZM in fruit juice samples based on third-order data generation. The data were obtained by following the time evolution, with an especially designed dispositive, of the EEFMs of the photolysis of AZM in alkaline medium. Then they were analysed with two well-known algorithms for second- and third-order data, PARAFAC and U-PLS/RBL-RTL. As will be shown, important findings regarding the second- and third-order advantages were observed and discussed.

2. Theory

2.1. Parafac

Four-way data arrays ($\boldsymbol{X}$) are obtained by arranging the third-order data of size $J \times K \times L$ for a set of I calibration samples, whose dimensions are $[(I+1) \times J \times K \times L]$. For PARAFAC modelling, it is of extreme importance that $\boldsymbol{X}$ follows a quadrilinear structure, which can be represented by Eq. (1) [32]:

$$X_{ijkl} = \sum_{n=1}^{N} a_{in} b_{jn} c_{kn} d_{\mathrm{ln}} + e_{ijkl} \quad (1)$$

where x_{ijkl} is an element of the four-way array of kinetic-excitation-emission fluorescence signals, a_{in} is the score of component n in sample i, N is the total number of responsive components, b_{jn}, c_{kn} and d_{ln} are the loading elements in the excitation, emission and time dimensions, respectively, and e_{ijkl} is an element of the array of errors not fitted by the model.

The model described by Eq. (1) defines a decomposition of $\boldsymbol{X}$ which provides access to excitation ($\mathbf{B}$) and emission spectral profiles ($\mathbf{C}$), kinetic profiles ($\mathbf{D}$) and relative concentrations ($\mathbf{A}$) of individual components in the $(I+1)$ samples, whether they are chemically known or not. An alternating least-squares minimization scheme is usually implemented for decomposition [33].

The initialization for the study of four-way arrays can be done using singular value decomposition (SVD) vectors, spectral data which are known in advance for pure components, or by the loadings giving the best fit after small PARAFAC runs involving both SVD vectors and several sets of orthogonal random loadings, options which can be implemented in the PARAFAC package.

PARAFAC performs a similar modelling for three-way data arrays ($\mathbf{X}$), which are obtained by arranging the second-order data of size $J \times K$ for a set of I calibration samples, whose dimensions are $[(I+1) \times J \times K]$.

2.2. U-PLS

U-PLS is an extended version of PLS algorithm, developed for first order data, which is capable of operating with higher orders. The cube-structured data for each sample are transformed into unidimensional arrays (vectors) by unfolding the original three-dimensional data. In the calibration step, the concentration information included in the vector $\mathbf{y}$ $(I \times 1)$ is employed, excluding data for the unknown sample [34]. This procedure allows to obtain a set of loadings $\mathbf{P}$ and weight loadings $\mathbf{W}$ ($JKL \times A$, where A is the number of latent variables) as well as regression coefficients $\mathbf{v}$ (size $A \times 1$). The parameter A is usually selected by the leave-one-out cross-validation procedure [35]. Subsequently, analyte concentration in unknown samples can be predicted with $\mathbf{v}$ using the following equation:

$$y_{\mathrm{u}} = \mathbf{t}_{\mathrm{u}}{}^{\mathrm{T}} \mathbf{v} \quad (2)$$

where $\mathbf{t}_{\mathrm{u}}$ (size $A \times 1$) is the unknown sample score, obtained by projection of the (unfolded) data for the test sample $\boldsymbol{X}_{\mathrm{u}}$ [vec($\boldsymbol{X}_{\mathrm{u}}$)] of size ($JKL \times 1$) onto the space of the A latent factors:

$$\mathbf{t}_{\mathrm{u}} = (\mathbf{W}^{\mathrm{T}}\mathbf{P})^{-1}\, \mathbf{W}^{\mathrm{T}} \mathrm{vec}(\mathrm{X}_{\mathrm{u}}) \quad (3)$$

It should be noted that if the sample under evaluation contains unexpected components, the scores given by Eq. (3) will generate abnormally large residuals in comparison with the typical instrumental noise (assessed by replicate measurements) when the prediction is performed using Eq. (2).

The effect of unexpected components in samples can be modelled with the RTL procedure through Tucker3 decomposition [30], i.e. by minimizing the norm of the residual vector $\mathbf{e}_{\mathrm{u}}$, computed while fitting the sample data to the sum of the relevant contributions to the sample signal. The expression for a single interference can be written as:

$$\mathrm{vec}(\mathrm{X}_{\mathrm{u}}) = \mathbf{P}\mathbf{t}_{\mathrm{u}} + g_{\mathrm{int}}(\mathbf{d}_{\mathrm{int}} \otimes \mathbf{c}_{\mathrm{int}} \otimes \mathbf{b}_{\mathrm{int}}) + \mathbf{e}_{\mathrm{u}} \quad (4)$$

where $\mathbf{b}_{\mathrm{int}}$, $\mathbf{c}_{\mathrm{int}}$ and $\mathbf{d}_{\mathrm{int}}$ are normalized profiles in the three modes for the interference and g_{int} is the first core element obtained for Tucker3 analysis of $\boldsymbol{E}\mathrm{p}$ in the following way:

$$(g_{\mathrm{int}}, \mathbf{b}_{\mathrm{int}}, \mathbf{c}_{\mathrm{int}}, \mathbf{d}_{\mathrm{int}}) = \mathrm{Tucker3}(\mathrm{E_p}) \quad (5)$$

The number of interferences N_{i} can be assessed by evaluating the final residuals s_{u} as a function of N_{i}, until s_{u} stabilizes at a value compatible with the experimental noise, allowing the location of the correct number of components.

For second-order data, the procedure called residual bilinearization (RBL) is applied in a similar way than RTL, but using SVD instead of Tucker3 analysis of the residual matrix $\mathbf{E}\mathrm{p}$ [16].

3. Materials and methods

3.1. Instrument

All spectrofluorimetric measurements were acquired on a Cary Eclipse fluorescence spectrophotometer (Agilent Technologies, Waldbronn, Germany) using a xenon flash lamp. The fluorescence measurements were made using a thermostated cell holder and an O.R.L., Hornos Eléctricos S.A. (Buenos Aires, Argentina) thermostatic bath.

Table 1
Predicted concentrations of azinphos-methyl in test samples ($\mu g\,L^{-1}$) containing the following non-modelled substances: FBZ ($0.5\,\mu g\,L^{-1}$), TBZ ($10.0\,\mu g\,L^{-1}$) and BTN ($10.0\,\mu g\,L^{-1}$).

Nominal	Second-order calibration		Third-order calibration	
	PARAFAC	U-PLS/RBL	PARAFAC	U-PLS/RTL
0.0 [a]	1.2 (0.5)	0.4 (0.3)	1.45 (0.03)	1.6 (0.3)
10.0	7.6	9.8	10.9	14.6
10.0	10.3	8.6	10.9	9.2
10.0	8.8	9.0	9.9	11.6
25.0	20.7	20.4	21.2	24.9
25.0	20.9	20.4	23.3	26.1
25.0	25.3	23.5	23.8	27.4
35.0	30.3	28.9	31.6	33.4
35.0	37.4	40.8	39.2	46.6
35.0	40.7	43.3	40.6	44.2
45.0	43.6	43.3	42.5	47.4
45.0	43.9	42.1	43.1	45.2
45.0	46.4	45.1	46.2	48.2
REP[b]	9	11	8	13
Slope analysis[c]				
Slope	1.02	1.01	0.98	1.04
S_R[d]	0.06	0.08	0.06	0.07
Number of samples (N)	13	13	13	13
t_{exp}[e]	1.2	0.5	1.2	2.1
t(0.025,11)	2.2	2.2	2.2	2.2

[a] Standard deviations between parenthesis.
[b] REP, relative error prediction in%.
[c] Hypothesis test: H_0 (Slope = 1) and H_a (Slope $\neq$ 1). Null hypothesis is accepted if t_{exp} < t (0.025, N-1).
[d] Standard deviations of slopes.
[e] Calculated as $t_{exp} = \frac{|1-Slope|\sqrt{N}}{S_R}$.

The UV-radiation source consisted in an Ocean Optics PX-2 pulsed xenon light source, with a spectral range between 220 and 750 nm. The light from the light source was transmitted through an optical fiber to the sample placed in the cuvette inside the spectrofluorometer. For this purpose, a custom-made cuvette holder was used, designed to hold a 1 cm square cuvette and to connect the optical fiber from the light source to the sample.

3.2. Chemicals and reagents

All standards were of analytical grade. Azinphos-methyl (AZM), fuberidazole (FBZ), thiabendazole (TBZ) and bitertanol (BTN) were provided by Sigma Aldrich (St. Louis, MO, USA). LC-grade methanol (MeOH) and acetonitrile (ACN) were obtained from Merck (Darmstadt, Germany). Chloroform ($CHCl_3$) was purchased from Cicarelli (Rosario, Argentina) and sodium hydroxide (NaOH) from Anedra (Buenos Aires, Argentina). Ultrapure water was obtained from a Milli-Q water purification system from Millipore (Bedford, MA, USA).

Stock standard solutions of AZM ($476.0\,mg\,L^{-1}$), TBZ ($700.0\,mg\,L^{-1}$), FBZ ($300.0\,mg\,L^{-1}$) and BTN ($500.0\,mg\,L^{-1}$) were prepared by dissolving accurately weighed amounts of each drug in MeOH and maintained the solutions under refrigeration at 4 °C in the dark. Working standard solutions were prepared by dilution of these solutions in Milli-Q water.

3.3. Calibration and test samples

A calibration set of five pure standard samples of AZM was prepared in triplicate by transferring appropriate aliquots of AZM working standard solution to 2.00 mL volumetric flasks and completing to the mark with Milli-Q water. The final concentrations were ranged between 0.0 and $70.0\,\mu g\,L^{-1}$.

Besides, a twelve-sample test set considering AZM concentrations different than those used for calibration (Table 1), and containing FBZ ($0.5\,\mu g\,L^{-1}$), TBZ ($10.0\,\mu g\,L^{-1}$) and BTN ($10.0\,\mu g\,L^{-1}$) as potential interferences was built.

Table 2
Predicted concentrations of azinphos-methyl in real samples ($\mu g\,L^{-1}$).

Fruit	Spiked	Found	
		PARAFAC	U-PLS/RTL
Apple	0	ND	ND
	150	186 (124)	120 (80)
	250	214 (86)	256 (102)
Peach	0	62 [a]	40 [a]
	120	99 (83)	111 (93)
	150	146 (97)	139 (93)
Pear	0	ND	ND
	200	233 (115)	202 (101)
	250	242 (97)	220 (88)
	Mean recovery (%)	101	93

[a] Detectable – not quantifiable concentration of AZM.
Between parenthesis: Recoveries (%).

3.4. Real samples

Apples, pears and peaches were purchased in the local market. The fruits were processed in a blender before submitting them to the extraction procedure. The standard addition calibration method was used in order to overcome the matrix effect, which involved spiking the real samples with three levels of AZM standard. Due to the matrix effect, the concentrations for the spiked samples were higher than those used for calibration in aqueous solution (Table 2). Nevertheless, in spite of this modification, the method remains appropriate to analyse these kind of samples, considering that the MRLs set by SENASA for AZM in fruits is $0.2\,mg\,L^{-1}$ [3].

In this work, the extraction consisted in a combination of dispersive liquid-liquid micro-extraction (DLLME) after QuEChERS acetonitrile extraction, and was adapted from a method previously reported in the literature [36]. QuEChERS technique (Quick, Easy, Cheap, Effective, Rugged and Safe), introduced in 2003 by Anastassiades et al. [37], combines an extraction step with acetonitrile followed by an extract clean-up using dispersive solid-phase extraction (d-SPE). On the other hand, DLLME is based on a ternary component solvent system in which an appropriate mixture of extraction and dispersive solvents is rapidly injected into an aqueous sample and a cloudy solution is formed [38]. In this work, the acetonitrile phase of QuEChERS extraction was used as the dispersive solvent for further DLLME. In the first step, 5.0 mL of ACN were added and mixed with 5.0 mL of fruit juice. Next, 2 g of $MgSO_4$ and 0.5 g of NaCl were added to allow, after centrifugation, the separation of water from the organic solvent. In the second step, 5.0 mL of Milli-Q water was placed in a centrifuge tube. Then, 2.0 mL of the ACN extract, previously obtained by QuEChERS extraction, and $200.0\,\mu L$ of $CHCl_3$ were rapidly injected into the 5.0 mL of water to form a cloudy solution. The samples were vortexed for 5 min and then centrifuged at 4000 rpm for 5 min. Finally, the sediment was removed using a syringe and collected in clean test tubes. The $CHCl_3$ was evaporated under a flow of nitrogen. The final residues were reconstituted with 2.0 mL of water and vortexed for 1 min.

3.5. EEM-kinetics procedure

The matrices were recorded in a 1 cm path length quartz cell. The readings were made in the excitation range of 220–320 nm every 5 nm, and emission range from 320 to 500 nm every 5 nm at a scan rate of $24{,}000\,nm\,min^{-1}$. The voltage of the photomultiplier detector was set to 600 V and the excitation and emission slits were

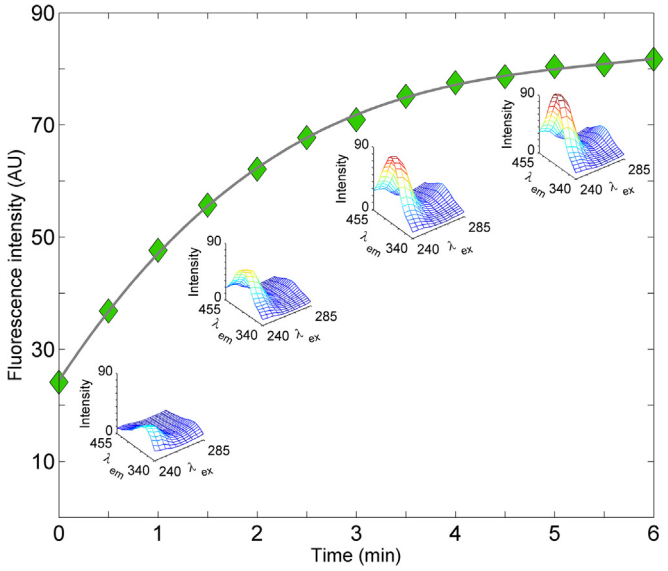

Fig. 1. Evolution of the fluorescence intensity of AZM (λ_{exc} = 240 nm; λ_{em} = 390 nm) and EEFM, as a function of time after irradiation.

both set to 10 nm. This criterion was applied to all the processed samples.

Third-order data were generated by measuring EEFMs at different irradiation times for each sample. The excitation and emission ranges in the matrices obtained were subsequently restricted in order to remove signal from Rayleigh dispersion.

3.6. Software

The Cary Eclipse software package was used to control the instrument, data acquisition and data analysis. The light source was controlled by the OceanView software.

All employed algorithms were implemented in MATLAB 7.6 [39]. A useful interface for data input and parameters setting written by Olivieri et al. [40], which can be downloaded from www.iquir-conicet.gov.ar/descargas/mvc3.rar, was employed for PARAFAC and U-PLS/RTL implementation.

4. Results and discussion

4.1. Data generation

The irradiation cycle was carried out at 25 °C on 2.0 mL of sample solution added with 20.0 μL of NaOH 1 mol L^{-1}. When a 0.025 mg L^{-1} AZM solution was analysed, the increment in the fluorescence intensity (registered at 240 nm in excitation and 390 nm in emission) was evidenced after two minutes and, after twenty minutes, a 15-fold increase with respect to the initial intensity was reached. Under these conditions, it was decided to achieve the photolysis in six min, which can be considered a reasonable period of time, an important fact when the system is used for a quantitative purpose and many measurements must be done for different sample solutions. Consequently, the reaction was set to be carried out in alkaline medium at room temperature for six minutes of irradiation, and registering EEFMs (of size 21 × 33 data points) every thirty seconds, i.e. 13 EEFMs per sample. Prior to data modelling, EEFM dimensions were adjusted in order to remove signal of Rayleigh dispersion, thus having 14 × 24 × 13 data points per sample.

Fig. 1 shows the evolution of the fluorescence intensity (λ_{exc} = 240 nm, λ_{em} = 390 nm) and the variation experimented in each EEFM as the reaction was progressing for the 0.025 mg L^{-1} AZM solution. As can be appreciated, changes in the landscapes corresponding to each reaction time are indicative of the gain in both selectivity and sensitivity when the time mode is exploited.

4.2. Three- and four-way calibration

At this point, the main objective of the present work was to demonstrate that augmenting the number of modes produces an increment in the predictive ability of the method, based on better both accuracy (as a result of the gain in selectivity) and sensitivity (as a consequence of using a large number of sensors). The latter fact was thoroughly discussed by Allegrini and Olivieri in Ref. [41]. In addition, it is of high importance in the chemometric community the discussion about if there is a third-order advantage when four-way calibration is implemented. In this regard, Wu and co-workers remarked that a third-order advantage could be associated with: a) the possibility of decomposing the data array for each sample exclusively, independent of other samples; b) the enhancement in sensitivity and selectivity; and c) the collinearity dismissing [42].

4.2.1. Analysis of test samples

Test samples were analysed applying two well-known algorithms, PARAFAC and U-PLS/RBL-RTL, to test the predictive ability of both models for AZM in the presence of unexpected compounds, and to study the comparative advantages of increasing the order of the data.

In order to model with PARAFAC, the data were arranged in two ways: a) second-order, using the last EEFM (obtained at time 6 min) for five pure standard samples of AZM (in triplicate) and the test sample, generating a three-way array of size [16 (samples) × 21 (excitation wavelengths) × 33 (emission wavelengths)]; and b) third-order, using the thirteen EEFMs registered at 13 times (each 30 s) for the 15 standards and the test sample, generating a four-way array of size (16 × 21 × 33 × 13).

For both second- and third-order calibrations, the first step in the PARAFAC modelling is the assessment of the correct number of sample constituents. This number was selected applying the so-called core consistency analysis (CORCONDIA) [43], resulting in four components. One of these components corresponds to the reaction product of AZM, and the other three belong to the interferences. The reason why a single component is retrieved for AZM is the following: although two chemical components occur in the calibration, they are mutually correlated because AZM is transformed into another compound. In addition, in one hand, there is a high similarity between the excitation and emission spectra of AZM and one of the interferences; and in the other, AZM presents an extremely low sensitivity (it almost does not present native fluorescence).

The non-negativity restriction was applied in all the modes. Fig. 2(A–C) shows the PARAFAC profiles obtained when modelling third-order data for excitation, emission and kinetics, juxtaposed with those obtained for pure standards. An interesting fact that can be appreciated by visual inspection of Fig. 2(A) is the large similarity among three of the four retrieved excitation profiles. These spectra correspond to the reaction product of AZM, and FBZ and TBZ. Fig. 2(C) shows the time profiles extracted by PARAFAC, being noticeable the evolution of the signal corresponding to the analyte (the reaction product of AZM), while the ones regarding to potential interferences remain constants. Based on the latter observation, it can be expected that adding an additional mode (evolution time) would provide an increasing in selectivity.

The U-PLS modelling was applied selecting the number of latent variables by the well-known leave-one-sample-out cross-validation procedure [35]. The optimum number of factors was estimated by calculating the ratios $F(A) = PRESS(A < A^*)/PRESS(A^*)$, where $PRESS = \Sigma(y_{i,act} - y_{i,pred})^2$, A is a trial number of factors and A^* corresponds to the minimum PRESS, and selecting the num-

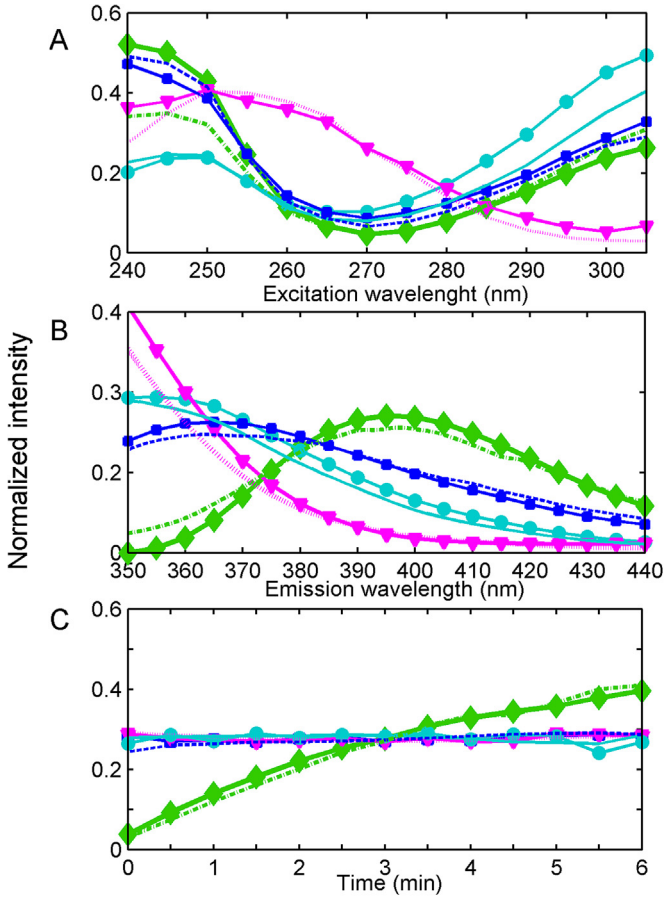

Fig. 2. Excitation (A), emission (B) and time (C) profiles obtained for a test sample by PARAFAC and for pure standards. PARAFAC/Pure standard profiles: AZM, green diamond/dash-dotted line; FBZ, cyan circle/continuous line; TBZ, blue square/dashed line; BTN, pink triangle/dotted line. (For interpretation of the references to colour in this figure legend, the reader is referred to the web version of this article.)

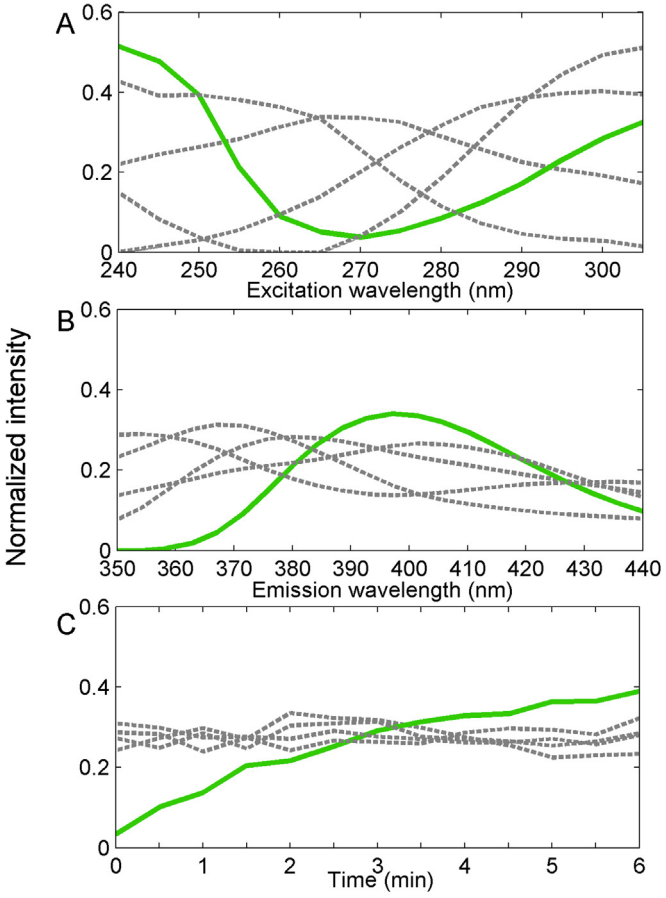

Fig. 3. Excitation (A), emission (B) and time (C) profiles obtained by PARAFAC for a real sample. AZM: green line, interferences: dashed grey lines. (For interpretation of the references to colour in this figure legend, the reader is referred to the web version of this article.)

ber of factors leading to a 75%-less probability that $F > 1$. Different to PARAFAC, the cross-validation procedure suggested two latent variables for AZM calibration, which can be attributed to AZM and the reaction compound, or to a high level of noise. On the other hand, RBL or RTL required two latent variables (N_i) in order to model the interference signals. As it was mentioned before, there is a high spectral similarity for two of the interferences, especially in the excitation mode, and this is why only two RBL/RTL components, instead of three, were required for the modelling. Nevertheless, as will be shown below, these two latent variables were enough to guarantee a good prediction in the test samples.

The selection of the number of potential interference substances (N_i) was based on the evaluation of the final residuals s_u as a function of N_i, until s_u (from Eq. (4)) stabilizes at a value compatible with the experimental noise. In the present case, and for the RTL procedure, when test sample #13 was evaluated, the residual decreased as follows: 77.5 ($N_i = 0$), 20.7 ($N_i = 1$), 11.9 ($N_i = 2$) and 9.5 ($N_i = 3$). The latter value, besides not showing a significant drop on the residual, furnished a bad prediction. Consequently, two potential interferences were considered for all the test samples.

Table 1 shows the results of predicted concentration for AZM and the recovery analysis performed in the test samples when second- and third-order calibrations were implemented. The slopes of the predicted vs nominal concentrations for each algorithm were calculated. A hypothesis test of whether the slope is significantly different from one was performed. Results obtained by application of both four-way approaches allowed us to conclude that the prediction of AZM in samples containing unexpected compounds was satisfactory in the conditions under study, taking into account that the best relative error prediction (REP) value was 8 for PARAFAC, and that the null hypothesis H_0: Slope = 1 was accepted at 95% confidence level in both cases. Moreover, these results suggest that the models are suitable to perform quantitative analysis in real samples, which may contain additional interfering compounds.

4.2.2. Real samples

Preliminary studies conducted in apple, peach and pear samples indicated that there was matrix effect due to intrinsic fruit components (data not shown). Therefore, the standard addition calibration method, which involved spiking three levels of standard to samples with and without the target analyte, was implemented.

Based on the better predictive results obtained when modelling four-way data (see above), only the latter were used for determination of the target analyte in real samples by application of both algorithms: PARAFAC and U-PLS/RTL.

For PARAFAC, the number of components used to model the data was 4 for apple and 5 for peach and pear. The non-negativity constraint was applied in the three modes. Fig. 3(A–C) shows the profiles obtained in the excitation, emission and kinetic modes, for the peach sample. Five different spectra can be observed in the excitation and emission profiles, one corresponding to AZM and the other four to interferences. This figure shows the complexity of the sample under analysis. On the contrary, in the temporal mode the fluorescent intensity increment is only observed for the target

Table 3
Analytical figures of merit for zero-, second- and third- order analyses in test samples.

Figure of merit	Zero-order	Second-order		Third-order	
		PARAFAC	U-PLS/RBL	PARAFAC	U-PLS/RTL
Sensitivity (AU μg^{-1} L)	14	24	10	77	32
$[\gamma^{-1}]$ ($\mu g\,L^{-1}$)[a]	7	0.05	0.2	0.02	0.2
LOD ($\mu g\,L^{-1}$)[b]	16	4.9	5.0	3.6	3.6
LOQ ($\mu g\,L^{-1}$)[c]	48	15	15	11	11

[a] Inverse of analytical sensitivity.
[b] LOD: Limit of detection, calculated according to [45].
[c] LOQ: Limit of quantitation, calculated according to [45].

analyte, while the others remain constant, which, such as in the case of the test samples, implies an important contribution to the selectivity of the method.

Owing to the fact that the standard addition method was used in this instance, the original data cannot be used for calibration modelling with U-PLS/RTL. This is because U-PLS requires the nominal analyte concentrations to be known, which are not available when building the calibration samples by spiking the analysed sample with known concentrations of the standard. However, there is a way in which U-PLS can be applied: if the data of the test sample are digitally subtracted from the data of the three standard additions and then three new virtual samples are created. The analyte response in these virtual samples is affected by the specific interactions with the background matrix, although the background signal has been removed by digital subtraction [44].

Table 2 presents the AZM prediction results for real samples analysed with PARAFAC and U-PLS/RTL. Mean recoveries above 80% were obtained for both models in the analysis of blank and two-level spiked samples for each fruit. It is interesting to mention that, although in concentrations lower than the limit of quantitation, AZM was detected in peaches. It should be highlighted that this limit is below the MRL established by SENASA and for this reason it can be certainly affirmed that, even though it cannot be quantitated, the amount of AZM residue in peach does not exceed the legal limit. On the other hand, no AZM residue was detected in apples and pears.

4.3. Figures of merit

Sensitivity is considered one of the most relevant figures of merit, from which others figures of merit can be estimated. Different approaches were used to define sensitivity and to extend this definition from univariate to multiway data. One of them defines sensitivity in terms of uncertainty propagation, as the degree of output noise from a system for a given input noise. This particular approach allowed to develop a general mathematical equation for sensitivity estimation comprising different degrees of data complexity and, in the case of multiway data, for different multiway algorithms [45].

Analytical figures of merit for both algorithms were calculated in test and real samples. Table 3 presents a comparison of the figures of merit obtained for zero-, second-, and third-order data in the analysis of the test samples. For zero-order, the fluorescence intensity in both the excitation and emission maximum of the AZM reaction product (λ_{exc} = 240 nm, λ_{em} = 390 nm) was registered at 6 min after irradiation, and the univariate calibration curve was evaluated following the IUPAC requirements [46]. For second-order analysis, the EEFM corresponding to the last irradiation time was considered for each sample. Finally, figures of merit for the EEFM-time third-order data were calculated. Sensitivity and limits of detection and quantitation show an improvement in the method when going from zero- to higher-order data. It can be seen that the limit of detection is five times lower in second-order modelling than in univariate calibration. In addition, as it was expected, the LOD is lower for third-order calibration. Although sensitivity is notably increased when going from second- to third-order calibration, this is not directly translated into lower limits of detection. The LOD decreases for increasing sensitivity, but it tends to level off at a certain point for higher sensitivities because of the contribution of a term independent of the sensitivity in the LOD calculation [41]. It can be seen that a substantial improvement is obtained when the data order is increased and, although in terms of predictive ability both models (three- and four-way) achieved similar results, figures of merit are enhanced in four-way calibration.

Table 4
Analytical figures of merit in real samples.

Fruit	Figure of merit	PARAFAC	U-PLS/RTL
Apple	Sensitivity (AU μg^{-1} L)	21	16
	$[\gamma^{-1}]$ ($\mu g\,L^{-1}$)[a]	0.2	0.8
	LOD ($\mu g\,L^{-1}$)[b]	48	30
	LOQ ($\mu g\,L^{-1}$)[c]	140	90
Peach	Sensitivity (AU μg^{-1} L)	38	40
	$[\gamma^{-1}]$ ($\mu g\,L^{-1}$)[a]	0.1	0.7
	LOD ($\mu g\,L^{-1}$)[b]	31	21
	LOQ ($\mu g\,L^{-1}$)[c]	93	63
Pear	Sensitivity (AU μg^{-1} L)	19	16
	$[\gamma^{-1}]$ ($\mu g\,L^{-1}$)[a]	0.2	1
	LOD ($\mu g\,L^{-1}$)[b]	66	51
	LOQ ($\mu g\,L^{-1}$)[c]	200	152

[a] Inverse of analytical sensitivity.
[b] LOD: Limit of detection, calculated according to [45].
[c] LOQ: Limit of quantitation, calculated according to [45].

Table 4 shows the figures of merit for the three analysed fruits. As it is expected, LOD and LOQ are higher than those achieved for the samples in aqueous solutions due to background matrix. LODs vary between 21 and 66 $\mu g\,L^{-1}$ depending on the sample, which is adequate in relation to the MRLs set by SENASA.

Finally, Table 5 presents a summary of the performance of different methods developed to analyse AZM in a variety of matrices. The comparison of the herein proposed method with those previously reported in the literature, allows us to highlight its advantages regarding sensitivity, selectivity and analysis time, among others. In general, they involve techniques that require sophisticated instrumentation, such as liquid chromatography coupled with tandem mass spectrometry or diode array detector, and gas chromatography coupled with tandem mass spectrometry. Although the LODs and LOQs obtained when using these methods are lower than those achieved in the present work, it is mandatory to consider that the sample extraction procedures include a pre-concentration step in most of the cases. Therefore, if lower limits of detection are necessary for a particular sample, the method presented in this report can be adapted by adding a pre-concentration step to the extraction procedure.

On the other hand, the use of third-order multivariate calibration, in contrast to the univariate calibration approach used in other methods for AZM quantitation, contributes significantly to the selectivity of the method. Specifically, the kinetic mode allowed to differentiate AZM from the interferences, not only those intentionally added to the samples to evaluate the second-order advantage but those unknown components present in the fruit matrix as well. This is of great importance, as the complex matrix of the fruit may present other components with fluorescence spectra similar to that of AZM and it could result difficult to quantitate AZM using EEFM second-order data.

Table 5
Comparison of the analytical performance of the proposed method with selected methods reported for the determination of AZM.

Method [a]	Real sample	Extraction [b]	Pre-concentration factor	LOD ($\mu g\,L^{-1}$)	LOQ ($\mu g\,L^{-1}$)	Ref
HPLC-DAD	Water	VLDS-SD-DLLME	80	0.2	0.6	[9]
LC-QqQ-MS/MS	Water	SPE	200	0.005	0.015	[10]
GC–MS/MS	Fruits	QuEChERS	–	NR[b]	2.0	[11]
GC–MS/MS	Cereals and animal feed	QuEChERS	–	NR[b]	50	[12]
GC-NPD	Fruits	MSPE	500	0.1	0.3	[13]
MEKC	Water	DLLME	40	5.0	NR[c]	[15]
PIF	Fruits	QuEChERS-DLLME	–	3.6	11	This work

[a] PIF: Photechemically induced fluorescence.
[b] VLDS-SD-DLLME: vortex-assisted low density solvent based solvent demulsified dispersive liquid– liquid microextraction; SPE: solid phase extraction; MSPE: magnetic solid phase extraction.
[c] NR: not reported.

5. Conclusions

In the present work, a simple, sensitive and accurate method for the determination of AZM in fruit juice samples based on excitation-emission-kinetic third-order data was developed. The generation of third-order data was achieved using simple instrumentation, i.e. a fluorescence spectrophotometer coupled to a UV-light source. Furthermore, the data acquisition was automated by the use of an optical fiber to transmit the UV radiation from the external light source to the sample in the spectrophotometer.

The data was successfully modelled using two algorithms, PARAFAC and U-PLS/RTL. The increment in data order allowed us to improve the analytical figures of merit, and the second order advantage made it possible to quantitate the target analyte in the presence of interferences, not only in test samples but in real fruit juice samples as well.

Acknowledgements

The authors are grateful to Universidad Nacional del Litoral (Projects CAI+D 2011 No. 11-11 and 11-7), CONICET (Consejo Nacional de Investigaciones Científicas y Técnicas, Project PIP-2015 No. 0111) and ANPCyT (Agencia Nacional de Promoción Científica y Tecnológica, Project PICT 2014-0347) for financial support. M.M. thanks CONICET for her fellowship.

References

[1] European Commission Pesticide MRLs – Regulation (EC) No. 396/2005, http://ec.europa.eu/food/plant/pesticides/eu-pesticides-database/.
[2] U.S. Department of Health & Human Services. U.S. Food and Drug Administration – Food Guidance & Regulation, http://www.fda.gov/Food/GuidanceRegulation/.
[3] Dirección Nacional de Agroquímicos, Productos Veterinarios y Alimentos del Senasa – Resolución-934-2010, http://www.senasa.gov.ar/normativas/.
[4] M. Ménager, X. Pan, P. Wong-Wah-Chung, M. Sarakha, J. Photochem. Photobiol. A: Chem. 192 (2007) 41–48.
[5] M. Bavcon Kralj, M. Franko, P. Trebse, Chemosphere 67 (2007) 99–107.
[6] P. Calza, C. Massolino, E. Pelizzetti, J. Photochem. Photobiol. A: Chem. 199 (2008) 42–49.
[7] L. Yeasmin, S.A. MacDougall, B.D. Wagner, J. Photochem. Photobiol. A: Chem. 204 (2009) 217–223.
[8] F. García Sánchez, A. Aguilar Gallardo, Analyst 117 (1992) 195–198.
[9] K. Seebunrueng, Y. Santaladchaiyakit, S. Srijaranai, Chemosphere 103 (2014) 51–58.
[10] A. Masiá, M. Ibáñez, C. Blasco, J.V. Sancho, Y. Picó, F. Hernández, Anal. Chim. Acta 761 (2013) 117–127.
[11] T. Portolés, L. Cherta, J. Beltran, F. Hernández, J. Chromatogr. A 1260 (2012) 183–192.
[12] S. Walorczyk, D. Drozdzynski, J. Chromatogr. A 1251 (2012) 219–231.
[13] S. Mahpishaniana, H. Sereshti, M. Baghdadi, J. Chromatogr. A 1406 (2015) 48–58.
[14] S. Mahpishanian, H. Sereshti, J. Chromatogr. A 1443 (2015) 43–53.
[15] P. Soisungnoen, R. Burakham, S. Srijaranai, Talanta 98 (2012) 62–68.
[16] A.C. Olivieri, Anal. Chem. 80 (2008) 5713–5720.
[17] G.M. Escandar, N.M. Faber, H.C. Goicoechea, A. Muñoz de la Peña, A.C. Olivieri, R.J. Poppi, TrAC Trends Anal. Chem. 26 (2007) 752–765.
[18] C. Kang, H.-L. Wu, L.-X. Xie, S.-X. Xiang, R.-Q. Yu, Talanta 122 (2014) 293–301.
[19] Y.J. Liu, H.L. Wu, C. Kang, C. Kang, H.W. Gu, J.F. Nie, S.S. Li, Z.Y. Su, R.Q. Yu, Anal. Sci. 28 (2012) 1097–1104.
[20] N. Rodríguez, M.C. Ortiz, L.A. Sarabia, Talanta 77 (2009) 1129–1136.
[21] R.P.H. Nikolajsen, K.S. Booksh, A.M. Hansen, R. Bro, Anal. Chim. Acta 475 (2003) 137.
[22] A. Muñoz de la Peña, I. Durán Merás, A. Jiménez Girón, Anal. Bioanal. Chem. 385 (2006) 1289–1297.
[23] A. Muñoz de la Peña, I. Durán Merás, A. Jiménez Girón, H.C. Goicoechea, Talanta 72 (2007) 1261–1268.
[24] A. Jiménez Girón, I. Durán-Merás, A. Espinosa-Mansilla, A. Muñoz de la Peña, F. Cañada añada, A.C. Olivieri, Anal. Chim. Acta 622 (2008) 94–103.
[25] S.H. Zhu, H.L. Wu, A.L. Xia, J.F. Nie, Y.C. Bian, C.B. Cai, R.Q. Yu, Talanta 77 (2009) 1640–1646.
[26] R.M. Maggio, P.C. Damiani, A.C. Olivieri, Anal. Chim. Acta 677 (2010) 97–107.
[27] P. Santa-Cruz, A. García-Reiriz, Talanta 128 (2014) 450–459.
[28] V.A. Lozano, A. Muñoz de la Peña, I. Durán-Merás, A. Espinosa Mansilla, G.M. Escandar, Chemometr. Intell. Lab. Syst. 125 (2013) 121–131.
[29] M.R. Alcaráz, G.G. Siano, M.J. Culzoni, A. Muñoz de la Peña, H.C. Goicoechea, Anal. Chim. Acta 809 (2014) 37–46.
[30] J.A. Arancibia, A.C. Olivieri, D. Bohoyo Gil, A. Espinosa Mansilla, I. Durán Merás, A. Muñoz de la Peña, Chemometr. Intell. Lab. Syst. 80 (2006) 77–86.
[31] X.-D. Qing, H.-L. Wu, X.-F. Yan, Y. Li, L.-Q. Ouyang, C.-C. Nie, R.-Q. Yu, Chemometr. Intell. Lab. Syst. 132 (2014) 8–17.
[32] C.M. Andersen, R. Bro, J. Chemometr. 17 (2003) 200–215.
[33] R. Bro, Chemometr. Intell. Lab. Syst. 38 (1997) 149–171.
[34] S. Wold, P. Geladi, K. Esbensen, J. Øhman, J. Chemometr. 1 (1987) 41–56.
[35] D.M. Haaland, E.V. Thomas, Anal. Chem. 60 (1988) 1193–1202.
[36] Y. Zhang, X. Zhang, B. Jiao, Food Chem. 159 (2014) 367–373.
[37] M. Anastassiades, S.J. Lehotay, D. Stajnbaher, F.J. Schenck, J. AOAC Int. 86 (2003) 412–431.
[38] M. Rezaee, Y. Assadi, M.R. Milani Hosseini, E. Aghaee, F. Ahmadi, S. Berijani, J. Chromatogr. A 1116 (2006) 1–9.
[39] MATLAB 7.6, The MathWorks Inc., Natick, Massachussets, USA, 2008.
[40] A.C. Olivieri, H.L. Wu, R.Q. Yu, MVC3: A MATLAB graphical interface toolbox for third-order multivariate calibration, Chemometr. Intell. Lab. Syst. 116 (2012) 9–16.
[41] F. Allegrini, A.C. Olivieri, Anal. Chem. 84 (2012) 10823–10830.
[42] H.-L. Wu, Y. Li, C. Kang, R.-Q. Yu, Multiway calibration based on alternating multilinear decomposition, in: A. Muñoz de la Peña, H.C. Goicoechea, G.M. Escandar, A.C. Olivieri (Eds.), Fundamentals and Analytical Applications of Multiway Calibration, Data Handling in Science and Technologyata Handling, 29, Elsevier, Amsterdam, 2015, Chapter 3.
[43] R. Bro, H.A.L. Kiers, J. Chemometr. 17 (2003) 274–286.
[44] V.A. Lozano, G.A. Ibañez, A.C. Olivieri, Anal. Chim. Acta 651 (2009) 165–172.
[45] A.C. Olivieri, Chem. Rev. 114 (2014) 5358–5378.
[46] A. Olivieri, Anal. Chim. Acta 868 (2015) 10–22.

Biographies

Milagros Montemurro Milagros Montemurro was born in Santa Fe, Argentina, in 1989. She graduated in 2013 as Licentiate in Biotechnology from National University of Litoral. Since then, she is performing a PhD in the Laboratory of Analytical Development and Chemometrics (LADAQ) at the National University of Litoral, in the Analytical Chemistry area. She received a doctoral research grant from the National Council of Scientific and Technical Research (CONICET) of Argentina. Her research interests include the development of analytical methods based on generation of higher order data applied to the quantitation of agrotoxics in fruits.

Gabriel G. Siano Gabriel G. Siano was born in Sunchales, Argentina, in 1981. He graduated in 2006 as Licentiate in Biotechnology and in 2013 he received his PhD in Biological Sciences from National University of Litoral in the Laboratory of Analytical Development and Chemometrics (LADAQ). He received doctoral and postdoctoral research grants from the National Council of Scientific and Technical Research (CONICET) of Argentina, and since 2015 he is a research assistant in that council. His research interests include Chemometrics and the development of open-source software/hardware for Analytical Chemistry.

María J. Culzoni María J. Culzoni was born in Rafaela, Santa Fe, Argentina, in 1979. She received her PhD from National University of Litoral (2008). After completing postdoctoral research at Universidad Nacional de Rosario, Argentina, she joined the faculty at National University of Litoral in 2010, where she is currently a teaching assistant of Analytical Chemistry and Chemometrics. Since 2010, she has been working as a researcher at the National Council of Scientific and Technical Research (CONICET) of Argentina. In 2013, she held a postdoctoral position in the School of Chemistry and Biochemistry at Georgia Institute of Technology in Atlanta, USA. Her research interests include the development of sensors and analytical methods based on fluorescence spectroscopy and separations coupled to efficient information extraction using chemometric modelling.

Héctor C. Goicoechea Héctor C. Goicoechea was born in Santa Fe, Argentina, in 1961. He received his PhD (2000) from the National University of Rosario. After completing postdoctoral research at Department of Chemistry and Molecular Biology, North Dakota State University, Fargo, USA, he joined the faculty at National University of Litoral, Santa Fe, in 2004, where he is currently a Full Professor of Analytical Chemistry and Chemometrics. He belongs to the National Council of Scientific and Technical Research (CONICET) of Argentina. His research interests include development of analytical methods based on fluorescence spectroscopy and separations coupled to chemometric modelling.